Title

The effect of radiation dose reduction on computer-aided detection (CAD) performance in a low-dose lung cancer screening population

Journal

Medical Physics, 44(4)

ISSN

0094-2405

Authors

Young, Stefano

Lo, Pechin

Kim, Grace

et al.

Publication Date

2017-04-01

DOI

10.1002/mp.12128

Peer reviewed

INTRODUCING

SunCHECK™

AUTOMATED AND INTEGRATED QUALITY ASSURANCE SOLUTIONS

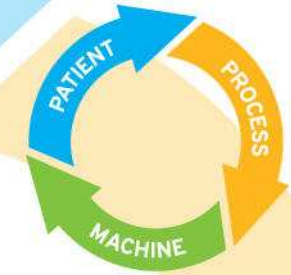

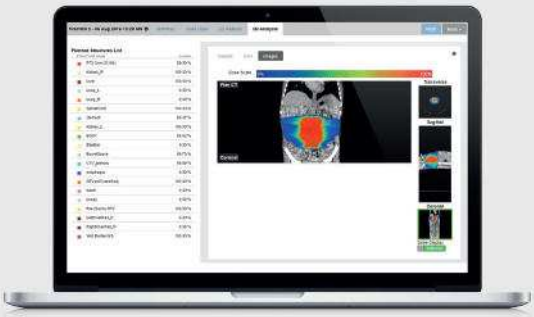

DoseCHECK™

Independent Secondary 3D Dose Calculations

Generate a full 3D dose volume to compare against a TPS-generated 3D dose volume, for verification of complex treatment fields.

PerFRACTION™

Fraction 0™ — 3D Pre-Treatment QA

Perform fully-automated phantom-less, EPID-based QA for independent measurement and analysis of 3D dose.

Fraction n™ — 3D In-Vivo Monitoring

Accurately and efficiently identify, isolate and understand the impact of set-up errors and anatomy changes on 3D dose deposited in the patient.

SNC Machine™

TG-142/VMAT Imaging and Mechanical QA

Automatically capture, process and analyze QA files, and save results to a database. Efficiently review, determine action and trend all data.

See what's next: sunnuclear.com/

SUN NUCLEAR corporation

Received Date: 08-Aug-2016

Revised Date: 16-Dec-2016

Accepted Date: 15-Jan-2017

Article Type: Research Article

The Effect of Radiation Dose Reduction on Computer-Aided Detection (CAD) Performance in a Low-Dose Lung Cancer Screening Population

Stefano Young[1a], Pechin Lo[1], Grace Kim[1], Matthew Brown[1], John Hoffman[1], William Hsu[1], Wasil Wahi-Anwar[1], Carlos Flores[1], Grace Lee[1], Frederic Noo[2], Jonathan Goldin[1], and Michael McNitt-Gray[1b]

1. Department of Radiological Sciences, University of California Los Angeles David Geffen School of Medicine, 924 Westwood Blvd, Los Angeles, California 90024.

Email addresses for correspondence: a) stefano.young@gmail.com, b) mmcnittgray@mednet.ucla.edu

2. UCAIR, Department of Radiology, University of Utah, 729 Arapeen Dr, Salt Lake City, UT 84108

Abstract

Purpose: Lung cancer screening with low-dose CT has recently been approved for reimbursement, heralding the arrival of such screening services worldwide. Computer-Aided Detection (CAD) tools offer the potential to assist radiologists in detecting nodules in these screening exams. In lung screening, as in all CT exams, there is interest in further reducing radiation dose. However, the effects of continued dose reduction on CAD performance are not fully understood. In this work, we investigated the effect of reducing radiation dose on CAD lung-nodule detection performance in a screening population.

Methods: The raw projection data files were collected from 481 patients who underwent low-dose screening CT exams at our institution as part of the National Lung Screening Trial (NLST). All scans were performed on a multi-detector scanner (Sensation 64, Siemens Healthcare, Forchheim Germany) according to the NLST protocol, which called for a fixed tube current scan of 25 effective mAs for standard-sized patients and 40 effective mAs for larger patients. The raw projection data were input to a reduced-dose simulation software to create simulated reduced-dose scans corresponding to 50% and 25% of the original protocols. All raw data files were reconstructed at the scanner with 1 mm slice

thickness and B50 kernel. The lungs were segmented semi-automatically, and all images and segmentations were input to an in-house CAD algorithm trained on higher-dose scans (75-300 mAs). CAD findings were compared to a reference standard generated by an experienced reader. Nodule- and patient-level sensitivities were calculated along with false positives per scan, all of which were evaluated in terms of the relative change with respect to dose. Nodules were subdivided based on size and solidity into categories analogous to the LungRADS assessment categories, and sub-analyses were performed.

Results: From the 481 patients in this study, 82 had at least one nodule (prevalence of 17%) and 399 did not (83%). A total of 118 nodules were identified. 27 nodules (23%) corresponded to LungRADS category 4 based on size and composition, while 18 (15%) corresponded to LungRADS category 3 and 73 (61%) corresponded to LungRADS category 2. For solid nodules ≥ 8 mm, patient-level median sensitivities were 100% at all three dose levels, and mean sensitivities were 72%, 63%, and 63% at original, 50%, and 25% dose respectively. Overall mean patient-level sensitivities for nodules ranging from 3 to 45 mm were 38%, 37%, and 38% at original, 50%, and 25% dose due to the prevalence of smaller nodules and non-solid nodules in our reference standard. The mean false-positive rates were 3, 5, and 13 per case.

Conclusions: CAD sensitivity decreased very slightly for larger nodules as dose was reduced, indicating that reducing the dose to 50% of original levels may be investigated further for use in CT screening. However, the effect of dose was small relative to the effect of the nodule size and solidity characteristics. The number of false positives per scan increased substantially at 25% dose, illustrating the importance of tuning CAD algorithms to very challenging, high-noise screening exams.

1. Introduction

The National Lung Screening Trial (NLST) demonstrated a reduction in lung cancer related mortality with lung cancer screening using low-dose CT [1]. As a result, this test has been approved for use in lung cancer screening [2] [3], and many institutions are expected to implement lung cancer screening programs. Computer-Aided Detection (CAD) tools may become an integral part of these screening programs, offering the potential to assist in detecting lung nodules from these screening exams. However, a challenge for CAD systems is the fact that the image acquisition systems are not static. New CT systems bring lower doses and novel reconstruction methods, which makes robustness to the CT system parameters especially important for any CAD tool in the clinical environment.

Research groups have employed various approaches to quantify and characterize the effects of CT dose on the nodule detection task. For example, Barrett et al. showed theoretical relationships between image quality and dose for different types of tasks. For an idealized detection task and a non-prewhitening model observer, ln(SNR^2) and AUC were shown to be asymptotically flat at high dose and drop off sharply in the limit of Dose -> 0 [4]. Das et al. investigated the performance of a lung-nodule CAD algorithm on images acquired at 100 effective mAs (“full dose”) as well as simulated 10 eff. mAs (“low dose”) images. They found, for nodules greater than 4mm, that “there was a statistically significant difference between the sensitivity of CAD at low dose and full dose” [5]. However, for all nodules, the difference was not statistically-significant, illustrating the impact of nodule size on CAD robustness. Christe et al. evaluated the performance of 3 different CAD algorithms on phantom images acquired over a range of settings from 120 kV, 100 mAs down to 80 kV, 25 mAs. Only one of the CAD

algorithms showed a statistically-significant loss of sensitivity at the lowest dose level ([6] – p. e874), illustrating that different CAD algorithms may respond to the dose differently. In another phantom study, Wielputz et al. concluded, "Nodule CAD on chest MDCT is robust over a wide range of exposure settings." [7] Only one of their settings (80 kV, 12 mAs) led to reduced CAD sensitivity.

The phantom and clinical studies above would seem to agree, qualitatively, with theory presented in [4]. However, they also suffer from a lack of analysis at dose levels expected to be used in current and future lung cancer screening programs. Radiation dose levels are already low for screening exams, and they are expected to continue to be reduced even further. Image noise is therefore expected to increase, making CAD detection of lung nodules challenging and potentially degrading CAD performance. The purpose of this work was to specifically investigate the effect of radiation dose reduction on CAD in terms of lung nodule detection in a screening population.

2. Methods

2.1 Patient cohort

First, we assembled a cohort of 481 patients who underwent low-dose CT scanning at our institution as part of the NLST, and for whom raw projection data was available. The availability of the original raw projection data was used as an inclusion criterion for this study, because it was a prerequisite for the reduced-dose simulations described in Section 2.2. All patients met NLST inclusion criteria for age, smoking history and physical condition [1]. All patients were scanned during the trial on a multi-detector CT (Sensation 64, Siemens Healthcare, Forchheim Germany) using the NLST protocol [8], which specified a fixed kV and effective mAs: 120 kV, 25 effective mAs for standard-sized patients, 40 effective mAs for large patients, pitch 1.0, rotation time 0.5 seconds, and collimation 64 x 0.6 mm. For each subject, raw projection data was exported from the scanner and archived on a large network share internal to our research group.

2.2 Simulated dose reduction

Simulated reduced-dose scans were generated using a previously-published noise addition model which involves modifying the quantum and electronic noise properties of the raw CT data directly, prior to the reconstruction step [9] [10]. The noise-addition software was applied to all of the original raw data files in parallel on our research cluster, and the total storage required for all of the original and reduced-dose raw data files was approximately 3 TB. Two simulated reduced-dose scans were created for each patient, corresponding to 50% and 25% of the original protocol. This corresponded to tube currents of 12.5 and 6.3 effective mAs (standard-sized patient), or doses of approximately 1 mGy and 0.5 mGy CTDIvol (32 cm phantom). The study protocols are summarized in Table 1. The simulated 25% dose level approximately corresponds to the minimum effective mAs supported by the scanner model in this study (6.3 effective mAs = 20 mA*0.5 sec rotation time/pitch 1.5).

Table 1 - Summary of the protocols (original and simulated reduced dose) used in this study.

Protocol	Effective mAs (std. sized subject)	mA	Approximate $CTDI_{vol}$ (32 cm phantom)
Original	25	50	2.0 mGy
Simulated 50%	12.5	25	1.0 mGy
Simulated 25%	6.3	12.5	0.5 mGy

2.3 Reconstruction

Reconstructions were performed by importing the original and simulated reduced-dose raw data files back to the original scanner where they were acquired. All of the images were reconstructed at 1 mm slice thickness using the medium-sharp B50 kernel. Figure 1 shows an example NLST patient at the original protocol, followed by simulated 50% and 25% dose scans.

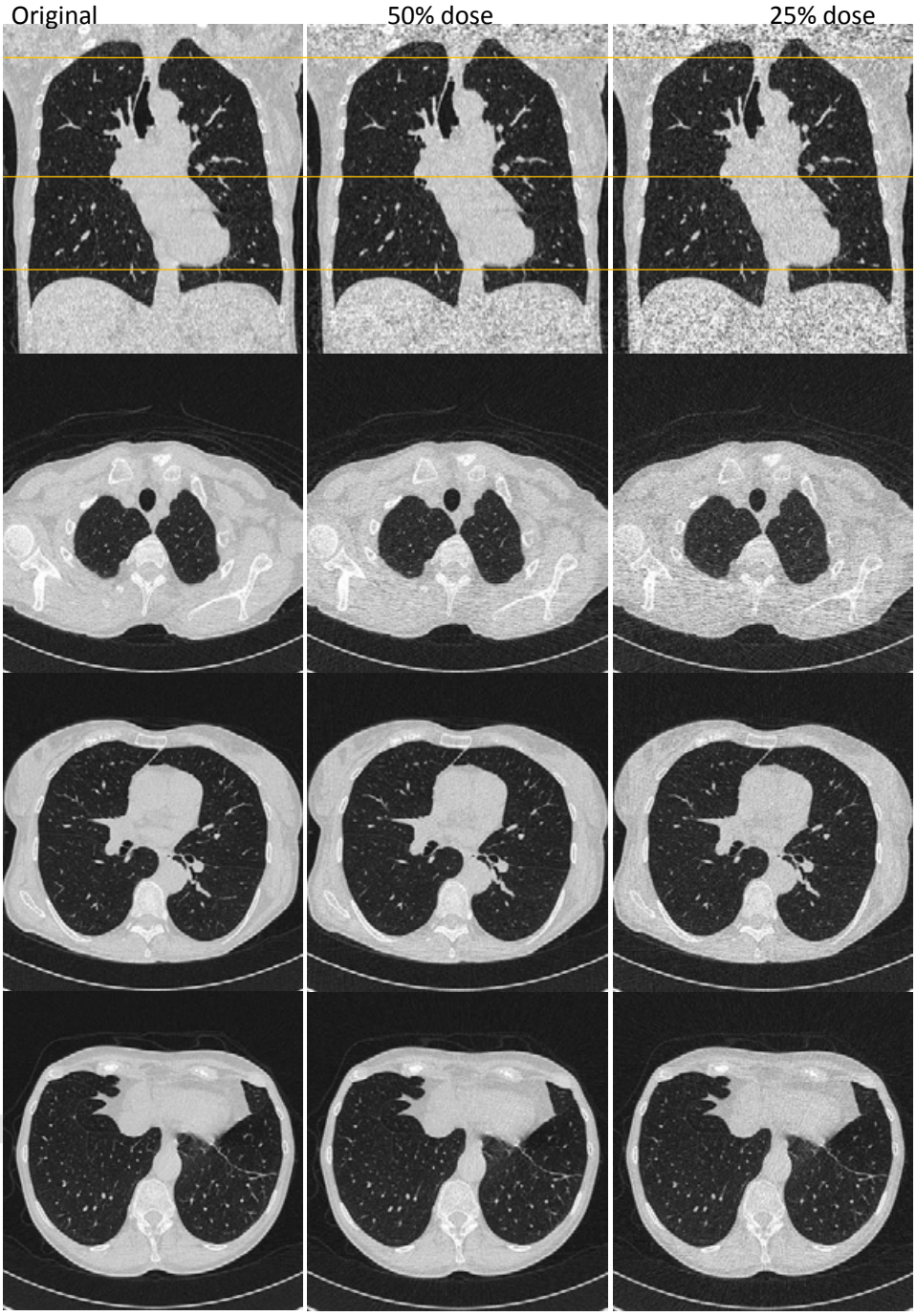

Figure 1 - An example screen-negative NLST patient at the original dose (left) followed by simulated 50% and 25% dose scans. Noise is pronounced in the shoulders and abdomen on the coronal views

Noise was particularly pronounced in the shoulders and abdomen due to the absence of tube-current modulation in the NLST protocol. Figure 2 shows an example of a larger patient at the original NLST dose, followed by the corresponding simulated reduced-dose images. The influence of patient size is evidenced by increased noise in the apices and bases of the lungs, particularly in the 25%-dose images.

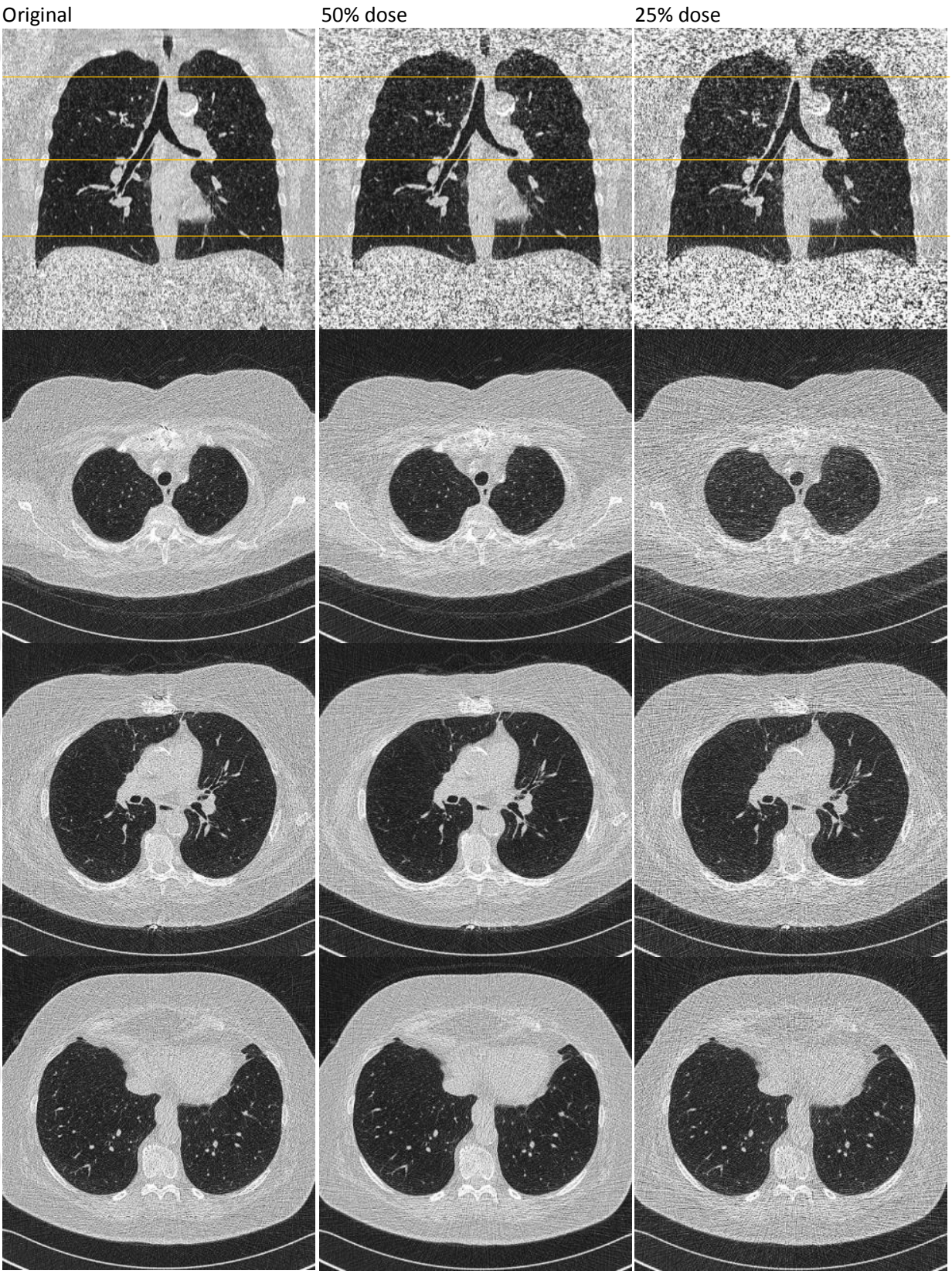

Figure 2 - An example of a larger screen-negative patient at the original NLST dose (left), followed by simulated 50% and 25% dose scans of the same patient. The noise is especially pronounced in the apices and bases of the lungs, as shown in the coronal views (top row).

2.4 CAD Algorithm

After simulating reduced-dose scans for all of the patients, we ran the cases through a semi-automated CAD algorithm. The first step was lung segmentation, which was performed using a seeded region-growing algorithm in MeVisLab software with threshold -600 HU. The seed was placed in the trachea on the original NLST image series, and the resulting segmentation (e.g. Figure 3) was also applied to the reduced-dose image series. The image series and lung segmentations for all patients were then input to a previously-published, in-house automated CAD software [11]. The version of the CAD in this experiment involved no smoothing or de-noising of the images.

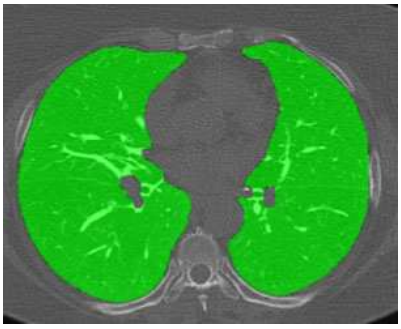

Figure 3 - Example lung segmentation result (overlayed in green) from MeVisLab seeded region-growing algorithm.

2.5 Assessing CAD Performance

To assess CAD performance, we used an existing reference standard generated by a single reader as part of the NLST. The reader was asked to specify the approximate slice number, anatomic location, and diameter of any nodules. The reader's findings were then used to mark the physical (x,y,z) locations of the nodules in MeVisLab software. In seven cases, the primary reader's notes were unclear and the authors could not locate the primary reader's findings, so a second expert chest radiologist with more than 20 years of experience was consulted to establish the reference standard for those cases. CAD results were compared to this reference standard at each dose level. Whenever a CAD marking overlapped with a reader finding, it was called a true positive. All other CAD markings inside the segmented lung volume were called false positives.

2.6 Analysis

The analysis involved three parts: (1) Nodule-level CAD sensitivity, where nodules were treated as independent samples (2) Patient-level CAD sensitivity, where patients were treated as independent samples, and (3) false positives per case. Mean nodule-level sensitivity, defined as total detections divided by total nodules, provides a reference for comparison with other CAD systems. Mean patient-level sensitivity, defined as detections divided by nodules per patient averaged over patients, is more relevant in a clinical context because nodules are not independent within a given patient. For each analysis, both means and medians were calculated, as the median better reflects the performance seen for a typical patient and is not as heavily influenced by outliers. For the sensitivity analyses, nodules were further separated based on their size and density characteristics using categories analogous to the LungRADS assessment categories: category 2 corresponded to solid nodules < 6 mm or non-solid nodules < 20 mm, category 3 corresponded to solid nodules ≥ 6 mm and < 8 mm or non-solid nodules ≥ 20 mm, and category 4 corresponded to solid nodules ≥ 8 mm [12]. Because the reader's annotations were recorded prior to the release of LungRADS, this classification had to be done retrospectively. Thus,

the nodules were reviewed and classified retrospectively by the authors using the reader's size measurements and descriptive findings text. Two-way analysis of variance was used to compare the mean patient-level sensitivities between dose levels and LungRADs categories. Scheffe multiple comparison tests were used to test the mean patient-level sensitivities of the LungRADs group by dose level.

3 Results

From the reference standard described in Section 2.5, readers identified that 82 of 481 subjects had at least one nodule (prevalence of 17%), while 399 did not have a nodule (83%). The total number of nodules was 118 with 60 subjects having only 1 nodule, 12 subjects having 2 nodules and 10 having > 2 nodules. This is summarized in Table 2. 73 (61%) of the nodules were classified as LungRADs category 2, 18 (15%) as LungRADs category 3, and 27 (23%) as LungRADs category 4. This is summarized in Table 3. This classification illustrates that many of the nodules were very low-contrast ground-glass nodules or micronodules; some examples of which are shown in Figure 4. Thus, the reduced-dose detection task was made even more difficult by a challenging set of nodules.

Table 2 - Patient characteristics in terms of numbers of nodules identified in the reference standard.

Total number of patients	481
No nodule identified	399 (83%)
At least 1 nodule	82 (17%)
1 nodule	60 (12%)
2 nodules	12 (2%)
> 2 nodules	10 (2%)

Table 3 - Nodule characteristics in terms of LungRADS categories.

Total number of nodules	118
LungRADs category 2	73 (61%)
LungRADs category 3	18 (15%)
LungRADs category 4	27 (23%)

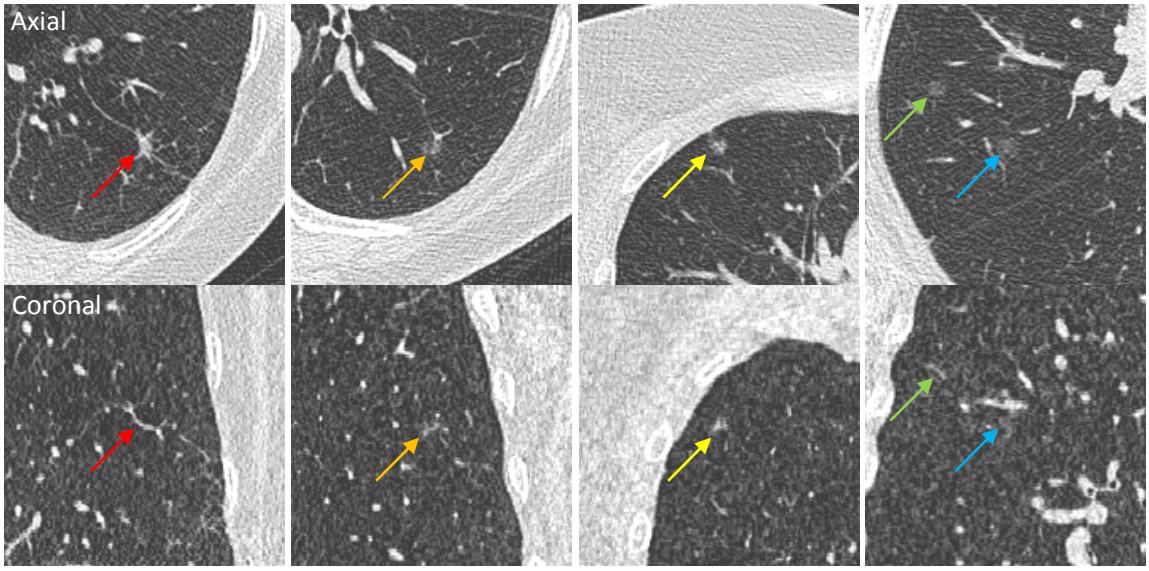

Figure 4 – Examples of challenging findings from our NLST reference standard which were classified as LungRADS category 2. All images are from the original NLST dose.

The median CAD sensitivity was 100% at all dose levels (Table 4) for the category 4 nodules, which ranged from 8-50mm in diameter with a mean of 13.6mm. Mean nodule-level sensitivities were significantly different between LungRADs categories ($p<0.001$), but not between dose levels ($p=0.85$). Mean sensitivities were 74.1%, 66.7%, and 66.7% at the original NLST dose, 38.9%, 27.8%, and 44.4% at 50% dose, and 21.9, 24.7%, and 26.0% at 25% dose respectively. Significant differences in the mean nodule-level sensitivity were found between LungRADs 4 and 3 at NLST and 50% dose levels ($p=0.033$ and $p=0.020$, respectively), but not at 25% dose ($p=0.29$) (Table 4). For nodules in categories 2 and 3, median sensitivity was zero and mean sensitivities ranged from 21.9 to 44.4%. Results were similar when treating the patients as independent samples (Table 5). In the Table 5 sub-analysis by category, N represents the number of patients with at least one nodule in that category. Overall patient-level mean sensitivities were 38.4%, 37.1%, and 37.7% for the original NLST dose, 50% dose, and 25% dose respectively.

Table 4 – Nodule-level sensitivity of CAD for each dose level. Values are reported by LungRADS category and pooled across all nodules.

Nodule-level CAD Sensitivity - Mean (Median) % Treating nodules as independent samples					
	Approx. CTDIvol [mGy]	LungRADs 4 Solid nodules ≥ 8 mm	LungRADs 3 Solid nodules ≥ 6 mm and < 8 mm or non-solid nodules ≥ 20 mm	LungRADs 2 Solid nodules < 6 mm or non-solid nodules < 20 mm	All nodules
		N=27	N=18	N=73	N=118
NLST Dose*	2.0	74.1 (100)	38.9 (0)	21.9 (0)	36.4 (0)
50% Dose**	1.0	66.7 (100)	27.8 (0)	24.7 (0)	34.7 (0)
25% Dose***	0.5	66.7 (100)	44.4 (0)	26.0 (0)	38.1 (0)

**: At NLST Dose level, p=0.033 between LungRADs 4 and 3; p<0.001 between LungRADs 4 and 2; p=0.34 LungRADs 3 and 2*
***: At 50% Dose level, p=0.020 between LungRADs 4 and 3; p<0.001 between LungRADs 4 and 2; p=0.97 LungRADs 3 and 2*
****: At 25% Dose level, p=0.29 between LungRADs 4 and 3; p<0.001 between LungRADs 4 and 2; p=0.32 LungRADs 3 and 2*
For all nodules, no statistically significant differences were found between dose levels (p=0.85).

Table 5 – Patient-level sensitivity of CAD for each dose level. Values are reported by LungRADS category and pooled across all nodules.

Patient-level CAD Sensitivity - Mean (Median) % Treating patients as independent samples					
	Approx. CTDIvol [mGy]	LungRADs 4 Solid nodules ≥ 8 mm	LungRADs3 Solid nodules ≥ 6 mm and < 8 mm or non-solid nodules ≥ 20 mm	LungRADs 2 Solid nodules < 6 mm or non-solid nodules < 20 mm	All nodules
		N=23	N=16	N=54	N=82
NLST Dose	2.0	71.7 (100)	37.5 (0)	24.4 (0)	38.4 (0)
50% Dose	1.0	63.0 (100)	25.0 (0)	29.3 (0)	37.1 (0)
25% Dose	0.5	63.0 (100)	43.8 (0)	26.2 (0)	37.7 (0)

Table 6 - CAD False Positives per scan for each dose level.

	Approx. CTDIvol [mGy]	False positives per scan Mean, Median (IQR)
NLST Dose	2.0	3.1, 2 (3)
50% Dose	1.0	5.1, 3 (4)
25% Dose	0.5	13.5, 6 (13)

The mean numbers of false positives per case were 3.1, 5.1, and 13.5, with medians of 2, 3, and 6 (Table 6). Interquartile ranges were 3, 4, and 13 for NLST dose, 50% dose and 25% Dose, respectively.

In Figure 5 is an example of a LungRADS 4 nodule from the reference standard, which was detected at the original NLST dose and missed at 50% and 25% dose levels.

Figu… vi… os… 25% …

Figure 6 shows a LungRADS 3 nodule, which was detected by the CAD at all three dose levels.

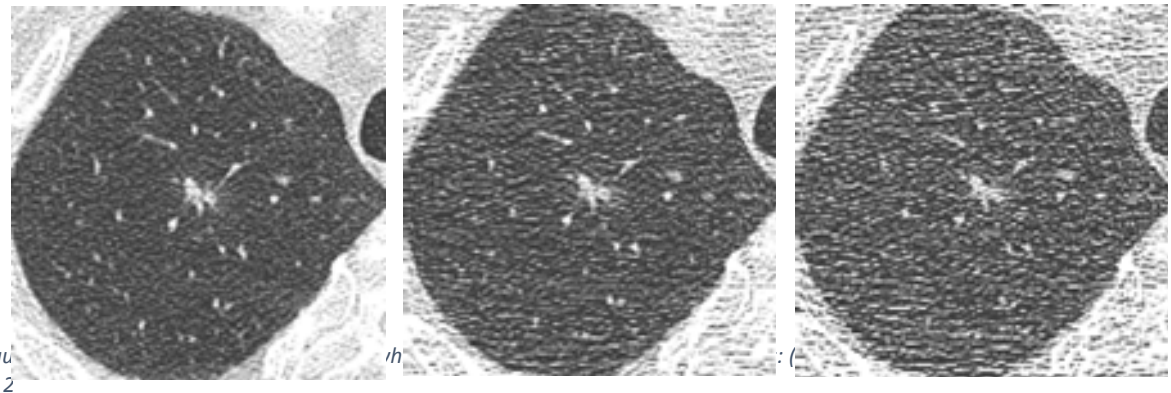

Figu h : (
(c) 2

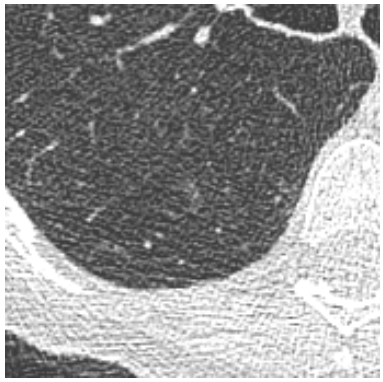

a b

Figure 7 - An example non-solid LungRADS 2 nodule which was missed by CAD at all three dose levels: (a) original NLST dose, (b) 50%, and (c) 25%.

Figure 7 shows a non-solid LungRADS 2 nodule, which was missed by CAD at all three dose levels.

Discussion

This work has demonstrated that, in the lung cancer screening context, reducing radiation dose had some relatively minor impact on CAD sensitivity, but this was small compared to the impact of the nodule characteristics, especially nodule size. Even at 25% of the NLST screening dose, or approximately 0.5 mGy, overall CAD sensitivity did not suffer the steep reduction in sensitivity that may have been anticipated. 25% of the NLST dose corresponds to tube currents of 6.3 mAs for standard-sized patients and 10 mAs for larger patients. Our results agree with the conclusions in [5], which were based on a similar low-dose t of 10 eff. mAs, but with olde -slice CT technology. The robustness of CAD sensitivity at these doses suggests that the theoretical detectability drop-off illustrated in [4] occurs more rapidly and at lower doses than the doses considered for this study.

Mean CAD sensitivity (patient-level) for solid nodules ≥ 8 mm decreased by 8.7% at reduced dose, but this decrease was relatively small compared to the changes in sensitivity for category 3 and category 2 nodules. Consider in Table 5, for example, the mean sensitivity difference at NLST dose between LungRADS categories 4 and 2: 47.3%. The factor 2 sensitivity drop between LungRADS categories 4 and 3 was likely due to the prevalence of non-solid nodules in category 3. In terms of

median sensitivity, dose had no impact on the CAD whatsoever. Nodule size and opacity clearly had a greater impact on the CAD sensitivity than the dose level. This is explained by the fact that the CAD algorithm was not specifically designed to detect ground-glass opacities, nor nodules less than four times the slice thickness (i.e. 4 mm). Due to the prevalence of category 2 and 3 nodules in our reference standard (76%), this presented an extremely challenging dataset for the CAD.

The CAD performance in this study differed from previously-reported results in [11] due to the difficulty of the dataset and reference standard that we chose. In [11], the authors used a publicly-available LIDC dataset consisting of higher-dose scans ranging from 75 to 300 mAs; 3 to 12 times the standard NLST protocol. Their reference standard was a four-reader consensus vote, as opposed to the single-reader-plus-consult paradigm in this study. In addition, they applied the criterion that all reference nodules must have dimensions ≥ 4 times the slice thickness, which was not strictly applied in this paper. The prevalence of solid nodules ≥ 8 mm (85%) was also much higher than in our study (23%, see Table 3).

Dose had a substantial impact on the average number of false positives. There were more than four times as many false positives at 25% dose than at the original NLST dose. As alluded to in [11], limiting false positives is a key factor in gaining widespread acceptance of clinical CAD systems. Our results suggest that care should be taken to tune the CAD algorithm to the dose at screening dose levels, in order to avoid sacrificing clinical utility. Since different scanners have different screening settings and noise properties, CAD systems may benefit from further scanner-specific tuning.

The radiation dose metric used in this manuscript was CTDIvol which, as has been noted elsewhere, is not patient dose [13]. This was used because it is the dose metric that CMMS has used in its guidelines on lung cancer screening [3] and is widely reported on CT scanners. Typical doses for NLST participants were reported in terms of both CTDIvol and effective dose [14]. However, since the NLST there has been substantial progress in developing dose metrics that take into account patient size (the Size Specific Dose Estimate or SSDE [15]) and on standardizing a patient size metric for that estimate (Water Equivalent Diameter as described in [16]). As SSDE and WED are not widely available yet on CT scanners (and were not available during the NLST), it is expected that CTDIvol will remain the dose metric of interest for the near future, especially as it is required to be reported by CMMS. Recently, Fujii et al. [17] reported CTDIvol and SSDE dose indices from the current clinical lung cancer screening program at UCLA. In the near future, we would expect reports regarding lung cancer screening and doses (e.g. values from the American College of Radiology's Dose Index Registry or ACR DIR [18]) to report both CTDIvol and SSDE.

Using raw data from the NLST was both an advantage and limitation of this work. It was advantageous in that we had access to a large raw data archive with well-defined screening protocols and an expert reference standard. However, the scans were performed on decade-old technology that has been superseded by newer scanners with tube-current modulation, improved detector efficiency, and better noise properties. The scanner in this work did not have iterative reconstruction capabilities, so our experiments were limited to conventional FBP reconstructions with a kernel similar to those used in the NLST.

Figure 8 shows three scans: original and simulated 25% dose scans of the same patient with NLST-era technology, followed by a different patient acquired from a more recent multi-detector CT (Force, Siemens Healthcare, Forchheim, Germany) with the same field of view and approximately the

same CTDIvol as the simulated 25% dose scan. This latest scanner offers several radiation dose reduction features common among recent CT scanners, including tube current modulation (CareDose4D [19]), advanced detector technology [20] and iterative reconstruction [21] [22]. In addition, it offers a unique capability for screening exams through the use of additional tin (Sn) filtration applied (Selective Photon Shield) which has previously been used for dual energy spectral separation [23], but in this scanner this addition filtration allows both fluence reduction and shaping of the polychromatic x-ray beam for reduced dose non-contrast scanning as is used in screening. The result is there is less noise overall at the same dose levels compared with previous generation MDCTs and the benefits of tube-current modulation are clearly visible in the apices and bases of the lungs.

These differences may translate to even better CAD performance at lower doses than indicated by our results, which may provide the potential for further dose reduction in screening. Therefore future work will include investigations into the effects of reducing radiation dose on CAD performance when these advanced technologies are used. In addition, it will be worth investigating the impact of slice thickness on the CAD system. The scanner model used in this study was limited to 0.6 mm slice thickness, and the reason we chose 1 mm was to be consistent with the standardized protocols used during the NLST. Reducing the slice thickness will increase the noise, which may not be an issue for solid nodules, but may well degrade the ability to detect ground glass or part-solid nodules. Looking into the LungRADs nodule subcategories and analyzing results by nodule size and type rather than LungRADS category is another area for further investigation.

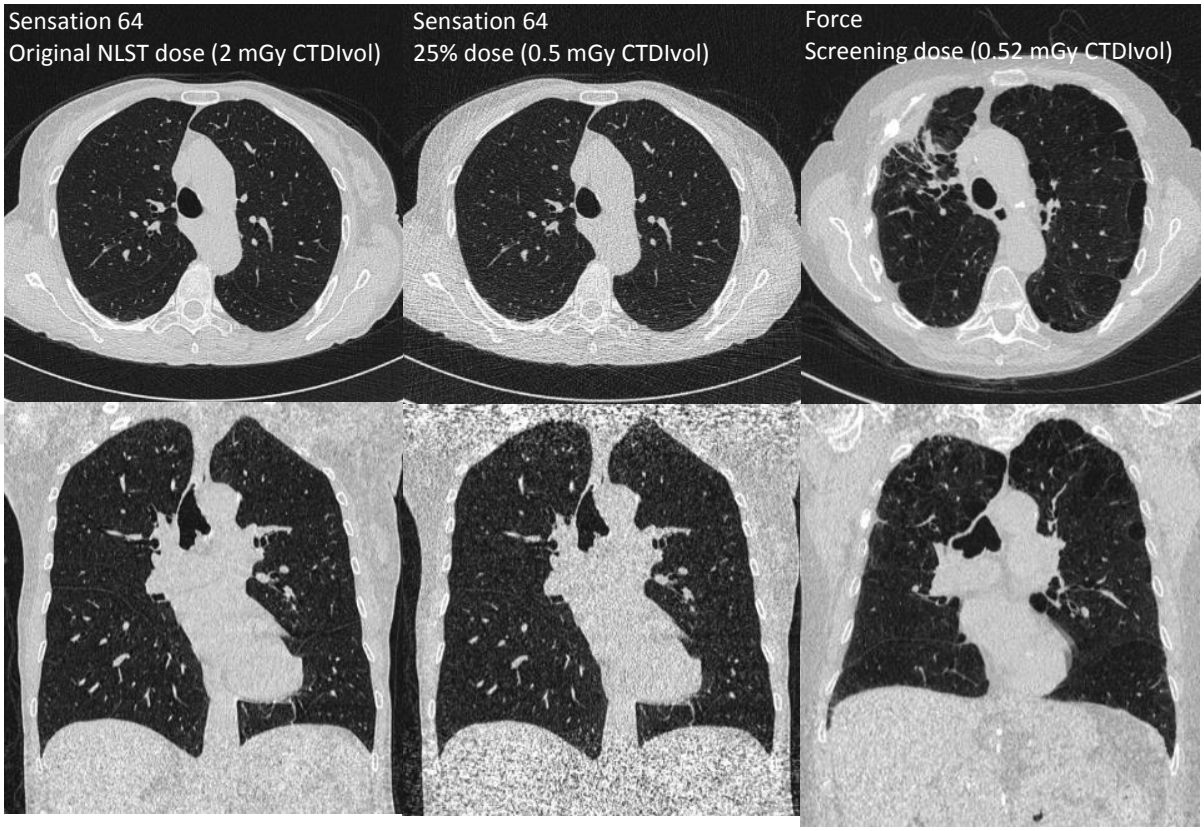

Figure 8 – Newer scanners may improve CAD robustness. The center and right columns both correspond to a quarter of the original NLST dose in the left column (approximately 0.5 mGy), but the right column has much less noise, in particular in the

apices and bases of the lungs on the coronal view, where tube-current modulation has a bigger impact. All images were reconstructed with a 310 mm FOV, 1 mm slice thickness, and W/L 1500/-400. The left and center columns were reconstructed with the B50 kernel, and the right column was reconstructed with the BR49 kernel.

Acknowledgements

Funding support for this research was provided in part by the University of California Office of the President Tobacco-Related Disease Research Program (UCOP-TRDRP grant #22RT-0131) and the National Cancer Institute's Quantitative Imaging Network (QIN grant U01-CA181156).

Disclosures

The UCLA Department of Radiological Sciences has an Institutional Master Research Agreement with Siemens Healthineers (formerly Siemens Healthcare, Erlangen, Germany).

References

[1] The National Lung Screening Trial Research Team, "Reduced Lung-Cancer Mortality with Low-Dose Computed Tomographic Screening," *The New England Journal of Medicine,* vol. 365, no. 5, pp. 395-409, 2011.

[2] United States Preventive Services Task Force, "Recommendations on Lung Cancer Screening using Low Dose CT," 31 December 2013. [Online]. Available: http://www.uspreventiveservicestaskforce.org/Page/Document/RecommendationStatementFinal/lung-cancer-screening. [Accessed 5 July 2016].

[3] Centers for Medicare & Medicaid Services, "Decision Memo for Screening for Lung Cancer with Low Dose Computed Tomography (LDCT) (CAG-00439N)," 5 February 2015. [Online]. Available: https://www.cms.gov/medicare-coverage-database/details/nca-decision-memo.aspx?NCAId=274. [Accessed 5 July 2016].

[4] H. H. Barrett, K. J. Myers, C. Hoeschen, M. A. Kupinski and M. P. Little, "Task-based measures of image quality and their relation to radiation dose and patient risk," *Physics in Medicine & Biology,* vol. 60, no. 2, pp. R1-R75, 2015.

[5] M. Das, G. Mühlenbruch, S. Heinen, A. H. Mahnken, M. Salganicoff, S. Stanzel, R. W. Günther and J. E. Wildberger, "Performance evaluation of a computer-aided detection algorithm for solid pulmonary nodules in low-dose and standard-dose MDCT chest examinations and its influence on radiologists," *British Journal of Radiology,* vol. 81, no. 971, pp. 841-847, 2008.

[6] A. Christe, L. Leidolt, A. Huber, P. Steiger, Z. Szucs-Farkas, J. E. Roos, J. T. Heverhagen and L. Ebner, "Lung cancer screening with CT: Evaluation of radiologists and different computer assisted detection software (CAD) as first and second readers for lung nodule detection at different dose levels," *European Journal of Radiology,* vol. 82, no. 12, pp. e873-e878, 2013.

[7] M. O. Wielpütz, J. Wroblewski, M. Lederlin, J. Dinkel, M. Eichinger, M. Koenigkam-Santos, J. Biederer, H.-U. Kauczor, M. U. Puderbach and B. J. Jobst, "Computer-aided detection of artificial pulmonary nodules using an ex vivo lung phantom: Influence of exposure parameters and iterative reconstruction," *European Journal of Radiology,* vol. 84, no. 5, pp. 1005-1011, 2015.

[8] C. H. Cagnon, D. D. Cody, M. F. McNitt-Gray, J. A. Seibert, P. F. Judy and D. R. Aberle, "Description and Implementation of a Quality Control Program in an Imaging-Based Clinical Trial," *Academic Radiology,* vol. 13, no. 11, pp. 1431-41, 2006.

[9] S. Zabic, Q. Wang, T. Morton and K. M. Brown, "A low dose simulation tool for CT systems with energy integrating detectors," *Medical Physics,* vol. 40, no. 3, p. 031102, 2013.

[10] S. Young, H. J. G. Kim, M. M. Ko, W. W. Ko, C. Flores and M. F. McNitt-Gray, "Variability in CT lung-nodule volumetry: Effects of dose reduction and reconstruction methods," *Medical Physics,* vol. 42, no. 5, pp. 2679-2689, 2015.

[11] M. S. Brown, P. Lo, J. G. Goldin, E. Barnoy, G. H. J. Kim, M. F. McNitt-Gray and D. R. Aberle, "Toward clinically usable CAD for lung cancer screening with computed tomography," *European Radiology,* vol. 24, no. 11, pp. 2719-28, 2014.

[12] American College of Radiology, "Lung-RADS Version 1.0 Assessment Categories," 28 April 2014. [Online]. Available: https://www.acr.org/~/media/ACR/Documents/PDF/QualitySafety/Resources/LungRADS/AssessmentCategories.pdf. [Accessed 19 May 2016].

[13] C. H. McCollough, S. Leng, L. Yu, D. D. Cody, J. M. Boone and M. F. McNitt-Gray, "CT dose index and patient dose: they are not the same thing.," *Radiology,* vol. 259, no. 2, pp. 311-6, 2011.

[14] F. J. Larke, R. L. Kruger, C. H. Cagnon, M. J. Flynn, M. F. McNitt-Gray, X. Wu, P. F. Judy and D. D. Cody, "Estimated radiation dose associated with low-dose chest CT of average-size participants in the National Lung Screening Trial," *Am. J. Roentgenol.,* vol. 197, no. 5, pp. 1165-9, 2011.

[15] American Association of Physicists in Medicine, "Size-specific dose estimates (SSDE) in pediatric and adult body CT examinations: the report of AAPM Task Group 204.," 2011. [Online]. Available: www.aapm.org/pubs/reports/RPT_204.pdf. [Accessed 23 Dec 2016].

[16] American Association of Physicists in Medicine, "Use of water equivalent diameter for calculating patient size and size-specific dose estimates (SSDE) in CT: the report of AAPM Task Group 220.," September 2014. [Online]. Available: www.aapm.org/pubs/reports/RPT_220.pdf. [Accessed 23 Dec. 2016].

[17] K. Fujii, K. McMillan, M. Bostani, C. Cagnon and M. F. McNitt-Gray, "Patient Size-Specific Analysis of Dose Indexes From CT Lung Cancer Screening," *AJR Am J Roentgenol.,* vol. 208, no. 1, pp. 144-149, 2017.

[18] K. Kanal, P. Butler, D. Sengupta and M. Bhargavan-Chatfield, "Diagnostic Reference Levels and Achievable Doses for Ten Commonly Performed US Adult CT Examinations from the ACR CT Dose

] Index Registry.," in *Radiological Society of North America 2016 Scientific Assembly and Annual Meeting*, Chicago, IL, 2016.

[19] C. H. McCollough, M. R. Bruesewitz and J. M. Kofler, Jr, "CT Dose Reduction and Dose Management Tools: Overview of Available Options," *Radiographics,* vol. 26, no. 2, pp. 503-512, 2006.

[20] X. Duan, J. Wang, S. Leng, B. Schmidt, T. Allmendinger, K. Grant, T. Flohr and C. H. McCollough, "Electronic Noise in CT Detectors: Impact on Image Noise and Artifacts," *American Journal of Roentgenology,* vol. 201, no. 4, pp. 626-632, 2013.

[21] F. Pontana, A. Duhamel, J. Pagniez, T. Flohr, J.-B. Faivre, A.-L. Hachulla, J. Remy and M. Remy-Jardin, "Chest computed tomography using iterative reconstruction vs filtered back projection (Part 2): image quality of low-dose CT examinations in 80 patients," *European Radiology,* vol. 21, no. 3, pp. 636-643, 2011.

[22] M. Beister, D. Kolditz and W. A. Kalendar, "Iterative reconstruction methods in X-ray CT," *Physica Medica,* vol. 28, no. 2, pp. 94-108, 2012.

[23] A. N. Primak, J. C. R. Giraldo, C. D. Eusemann, B. Schmidt, B. Kantor, J. G. Fletcher and C. H. McCollough, "Dual-Source Dual-Energy CT With Additional Tin Filtration: Dose and Image Quality Evaluation in Phantoms and In Vivo".